



Degradation of Methylene Blue by Pulsed Nanosecond Discharge in Water with Ar-O₂ Gaseous Bubbles

Nadir Aloui^{1,2} · Julien Pregent^{3,4} · Camille Gouze¹ · Ibtissem Belgacem² · Ahmad Hamdan¹

Received: 11 December 2023 / Accepted: 27 March 2024 / Published online: 9 April 2024

© The Author(s), under exclusive licence to Springer Science+Business Media, LLC, part of Springer Nature 2024

Abstract

The rise of water effluents containing emerging contaminants that resist conventional chemical and physical treatments makes the treatment of wastewater more complex. Plasma-based treatment methods have great potential to degrade many of the emerging contaminants, including dyes. In this study, using pulsed nanosecond discharges, we investigate the degradation of methylene blue (MB) dye in water by generating plasma in Ar-O₂ gas bubbles in water. The scalability of the setup is studied by producing discharges in a one electrode setup (a needle-to-plate configuration) and in a four electrodes setup (four needles-to-wire configuration). The discharge was characterized by electrical measurements (current and voltage waveforms) and optical emission spectroscopy. We find that the discharge properties are stable during the 30 min of processing, with and without the presence of MB in solution at low electrical conductivity. The production rate of H₂O₂ in the one electrode setup was measured in 0% and 70% O₂, and it was found to be ~2.3 and 2.9 mg/Lmin, respectively. In the four electrodes setup, H₂O₂ production rate was lower: ~1.2 and 1.9 mg/Lmin in 0% and 100% O₂. Degradation of MB was assessed in both setups for (i) different % of O₂ in the gas mixture, (ii) different MB initial concentration, and (iii) different initial water conductivity. In the one electrode setup, a high MB degradation (>85%) was generally achieved in all conditions, but a better performance is noted in high O₂ percentage (>50%) at low initial water conductivity. At low MB concentration and low electrical conductivity, the performance of the four electrodes setup was better than the one electrode setup.

Keywords Plasma in bubbles · Nanosecond discharge · Degradation of methylene blue · Scale up

Introduction

In recent decades, wastewater treatment has become more complex because of the rise of water effluents containing so-called “emerging” contaminants that resist conventional chemical and physical treatments. Amongst those are dye-based contaminants that do not

Extended author information available on the last page of the article

degrade easily and can have a harmful impact on health and environment [1, 2]. Recently, plasmas have been proposed as a solution for wastewater treatment [3–9]. Their advantage resides in the generation of reactive oxygen species (ROS), either in the gas or liquid phase [10–13], that can successfully degrade persistent contaminants in water.

Different systems have been reported to generate plasma-water interactions. Plasma can be produced directly in water [14, 15], generally by immersing two electrodes. While this method is simple and produces ROS directly in water, it requires high energy to break down water molecules [16], as well as specific power supplies. In other systems, the plasma is produced in the gas phase in the vicinity of the solution [9, 13, 17], and the plasma reactive species are then mixed with the liquid by diffusion or gas flow. While they are relatively simple, these systems are limited by the relatively low penetration of plasma species in water volume. A hybrid system that can enhance the interaction between the plasma species and the solution consisted of injecting gas/plasma bubbles in the water [18–21]. This method has the advantages of both previous systems, i.e. (i) it is produced in gaseous bubbles (i.e. low breakdown voltage) [22], (ii) it is in solution (high diffusion rate of reactive species via the gas-/plasma-liquid interface) [23], and (iii) it is tunable in terms of plasma chemistry (adjustable gas composition) [19, 21, 24–27]. Therefore, such systems showed excellent results for removing contaminants from solution [8, 24, 25]. However, the dynamics of plasma-water interactions and the complex chemical kinetics involving species in gas, in solution, and at the interface are not yet fully understood.

In the continuity of exploring the application of the plasma-bubbles configuration in water processing, addressing the role of gas composition on the discharge characteristics as well as on the removal of contaminants is crucial. In a previous study [24], the influence of gas composition, Ar, O₂, or N₂, is addressed. The discharge properties depend on the gas composition as well as on the plasma processing time, particularly in the case of N₂, as water electrical conductivity increased significantly. Also, the highest efficiency of methylene blue (MB) degradation was obtained in O₂ plasma gas, while the lowest was obtained in N₂; an intermediate efficiency was obtained in Ar. While the MB degradation can be linked to the formation of ROS (mostly OH radicals, but also H₂O₂ and O₃) either in gas, in solution, or at the interface, the kinetics driving its generation can be radically different in different gas composition. With Ar, it is expected that OH radicals are produced by electron-induced dissociation of water molecule ($e + \text{H}_2\text{O} \rightarrow \text{OH} + \text{H} + e$). With O₂, the reaction kinetics are expected to be much more complex by involving several species (O₂, O, O₃, H₂O₂, etc.) and creating different pathways for radicals' production.

This study is a follow-up of the previous work [24]. Herein, we focus on Ar-O₂ gas mixtures to determine its effect on the discharge characteristics as well as on the efficiency of MB degradation. The interest lies in observing whether the efficiency of MB degradation is affected by combining a gas with a lower ionization threshold (i.e. Ar) and another gas that can generate a lot of ROS (i.e. O₂). The plasma characteristics are determined by electrical and optical emission spectroscopy measurements. Towards the scale up of the process, the system of one electrode is replaced by a set of four similar electrodes. This novel configuration was characterized, and the efficiency of both systems to degrade MB are determined.

Experimental Setup

The experimental setup shown in Fig. 1 is used to produce discharges in gaseous bubbles in water. The discharge is produced using a nanosecond negative polarity pulsed power supply (NSP 120-20-N-500-TG-H, Eagle Harbor Technologies) at an amplitude of -20 kV, a pulse width of 500 ns, and a repetition rate of 1 kHz. The high voltage was connected to a hollow-needle-like (inner and outer diameters of 0.3 and 0.5 mm, respectively) mounted at the bottom of the discharge cell, whereas the ground was connected to a stainless-steel disc (diameter of 2 cm) mounted at the top of the discharge cell. The interelectrode gap distance was fixed at 8 mm, and the electrode assembly was mounted in a 10-cm-long cylindrical quartz cell with inner and outer diameters of 3.0 and 3.2 cm, respectively. The cell was filled with 200 mL of water at various electrical conductivity. This latter has been adjusted between 5 (deionized water) and 200 $\mu\text{S}/\text{cm}$ using KCl. Mass flow controllers were used to inject Ar and O_2 (purity of 99.99%) gas mixture at different percentage into the liquid through the lower hollow needle. The total gas flow rate was fixed at 1 L/min, resulting in a continuous array of bubbles with an average diameter of ~ 1 mm. Note that, under similar voltage conditions, discharges cannot occur without bubbles.

The electrical characteristics of the discharges were acquired using an oscilloscope (MSO54, Tektronix). The voltage was measured using a high-voltage probe (P6015A, Tektronix), whereas the current was measured using a current monitor (6585, Pearson). Since the oscilloscope cannot acquire waveforms at frequencies as high as 1 kHz, the frequency of the discharge was lowered to few Hz for a few seconds, and 50 successive waveforms were acquired. Note that the electrical waveforms were monitored during the whole processing time, and there was no significant difference between the low- and the high-frequency cases, i.e. no change in the discharge mode.

Production of ROS by the discharge was characterized by measuring the concentration of H_2O_2 . The concentration was measured in deionized water processed by the plasma using drop count titration method based on Sodium Thiosulfate titrant. In this technique a sample of 30 mL is taken in which we add 1 mL of Ammonium Molybdate and Sulfite Reagent Powder to get dark purple solution. From the prepared solution we take ~ 6 mL and care-

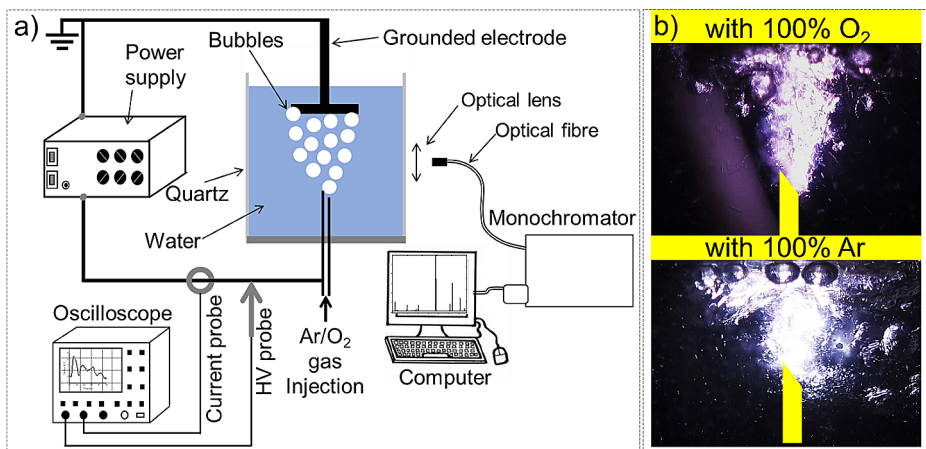


Fig. 1 Scheme of the experimental setup

fully add the Thiosulfate titrant drop by drop until the color of the solution becomes clear. The number of drops to get clear solution allowed the determination of H_2O_2 concentration. The uncertainty on the measured values are determined statistically by conducting multiple measurements at a given condition; an uncertainty of ± 2 mg/L on the measurements was applied.

Methylene blue (MB) at 5, 10, or 20 mg/L was utilized as a representative organic contaminant, and its degradation rate induced by plasma processing has been monitored using UV–visible absorption (Cary 5000 UV–Vis–NIR, Agilent) spectrophotometer. More precisely, we monitored the evolution of the peak intensity at 664 nm, as its absorbance intensity is representative to the presence of MB in solution. The acidity and conductivity of processed solution were measured using a pH meter (VWR Symphony SB20) and conductivity meter (19101-10 Digital Conductivity Meter, Cole-Parker Instrument), respectively.

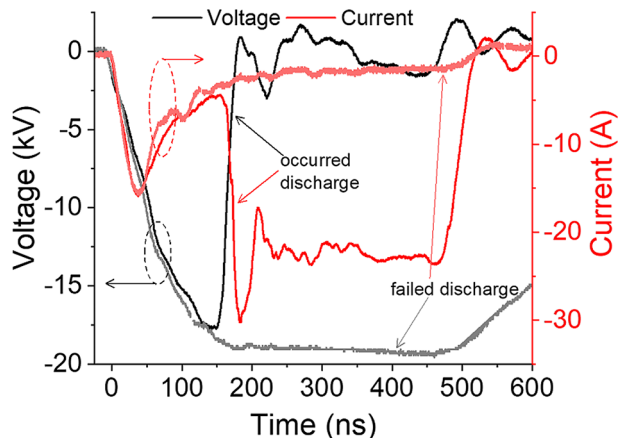
Results

Characteristics of the Discharge

Voltage and current waveforms are acquired every 1 min of processing. The waveforms for a typical discharge in water with 70% O_2 (and 30% Ar) are shown in Fig. 2; in the same figure, we add the waveforms for a non-occurred discharge. In this example, we identify the breakdown moment at ~ 150 ns, and it corresponds to voltage drop and current peak. As compared to the waveforms of a non-occurred discharge, some difference in the voltage rising period is noticeable. Such a difference can be related to the discharge ignition in bubbles before it transitions to a spark. In the following, the acquired waveforms are processed using a home-made algorithm to determine breakdown voltage, current peak, and discharge delay.

Before presenting the influence of different experimental parameters on the electrical characteristics, we compare the breakdown voltage (Fig. 3a) and the discharge current (Fig. 3b) for discharges in deionized water with Ar bubbles with and without MB during 30 min of processing. These figures clearly show that the MB did not influence the discharge characteristics. Although the results presented in Fig. 3 correspond to Ar bubbles,

Fig. 2 Voltage-current waveforms for a typical discharge in deionized water



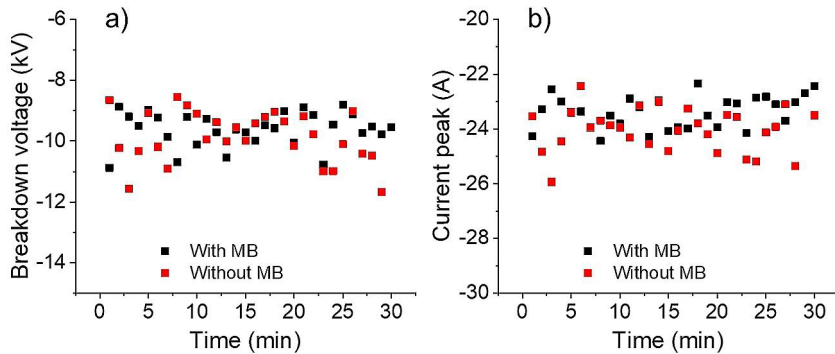


Fig. 3 Evolution of **a)** breakdown voltage and **b)** discharge current as a function of plasma processing time of deionized water without and with MB (10 mg/L)

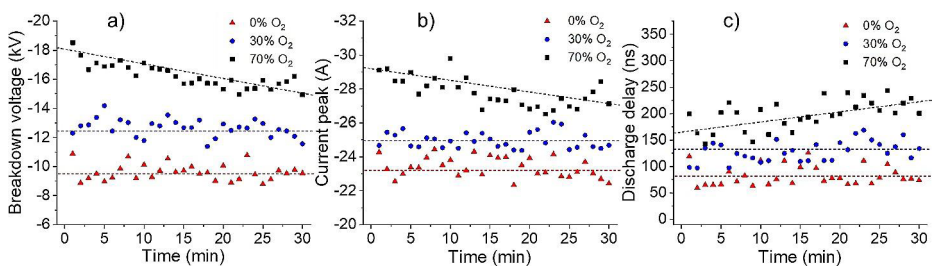


Fig. 4 Evolution of **a)** breakdown voltage, **b)** discharge current, and **c)** discharge delay as a function of plasma processing time of deionized water with MB (10 mg/L) under different conditions of O₂ percentage in Ar: 0%, 30%, and 70%

discharges with other bubbles composition were also performed, and the results were similar to the previous ones.

Figure 4a and b, and c show the temporal evolution of breakdown voltage, discharge current, and discharge delay, respectively, as a function of plasma processing time with different percentage of O₂ in Ar. In the case of 0% O₂, we remark that the breakdown voltage does not significantly change with the processing time and remains around -9 ± 1 kV. Concerning the discharge current, we measure values around -23 ± 1 A during the 30-min of processing. The discharge delay of the majority of the discharges varies between 50 and 100 ns, which indicates that they occur in the rising period of the high voltage pulse. In the case of 30% O₂, similar trends are noticeable with higher breakdown voltage (-12 – -14 kV), higher discharge current (-24 – -26 A), and longer discharge delay (100–150 ns). At 70% O₂, the breakdown voltage is also relatively higher, but interestingly it decreases linearly with the processing time. Initially, we measure ~ 18 kV, and it decreases to ~ 15 kV after 30 min of processing. This trend is also visible for the discharge current, and it decreases by ~ 2 A (from ~ 29 to -27 A) after 30 min of processing. As for the discharge delay, it increases by ~ 50 ns (from ~ 175 to 225 ns). These values indicate that the discharges in this condition of 70% O₂ occur in the beginning of the plateau period of the high voltage pulse. Note that measurements at higher %O₂ were also performed, and the values are found close to those

at 70% O₂. The results reported in Fig. 4 indicate two facts: (i) the add of O₂ in Ar induces an increase in the breakdown voltage, and (ii) at high O₂ content, the discharge characteristics evolve with processing time. The increase of breakdown voltage can be explained by the loss of electrons by attachment to O and O₂ to form O⁻ and O₂⁻, respectively. It has been demonstrated that this attachment process induces an increase in the reduced critical E-field strength from ~20 to 120 Td as the O₂ content in Ar increases from 0 to 100% [28]. For instance, the increase of O₂ content from 30 to 70% induces an increase in the reduced critical E-field strength from ~80 to 120 Td, i.e. a factor of 1.5. This ratio agrees well with the measured breakdown voltage ratio (at 0 min) which is ~18/12=1.5. The decrease of the breakdown voltage with the processing time is probably due to the enrichment of water with ionic species, as evidenced by the increase of water electrical conductivity from ~5 to 50 μS/cm after 30 min of processing (Figure S1 in Supplementary Material). The presence of these species in water induces a decrease of the plateau value (due to the dissipation of the power by ions displacement under the action of E-field) and not a decrease in the critical electric field strength. This is further supported by the increase of the discharge delay, i.e. the discharges occur later in the pulse.

Figure 5a and b, and c show the temporal evolution of breakdown voltage with various MB concentrations, namely 5, 10, and 20 mg/L, under different content of O₂: 0%, 30%, and 70%. At 0 and 30% of O₂, we observe that the breakdown voltage did not evolve with the processing time, and the average values are ~-10 and -14 kV, respectively. In the case of 70% of O₂, as mentioned earlier, the breakdown voltage decreases with the processing time. The decrease (from ~-18 to -15 kV after 30 min of processing) is similar at 5 and 10 mg/L of MB. However, at 20 mg/L of MB, we remark that the decrease rate of the breakdown voltage is much higher: it decreases linearly from ~-18 to -10 kV after 30 min of processing. In general, the decrease of breakdown voltage is related to the increase of water electrical conductivity that induces a lowering of the pulse plateau value. The more significant decrease of voltage at 20 mg/L may be related to higher concentration of ionic by-products in water.

Figure 6 shows the evolution of optical emission spectra as a function of plasma processing time for two O₂ content: 0% (Fig. 6a) and 70% (Fig. 6b). The spectra indicate the presence of Ar, H, and O lines. Ar lines originate from the gaseous bubbles, H line originates from water dissociation, and O lines originate from both water dissociation (at 0% O₂) and gaseous bubbles. With O₂ (at 30 and 70%), the spectra are dominated by O at 777 nm, while it is the Ar line (at 811 nm) in the case of 0% O₂.

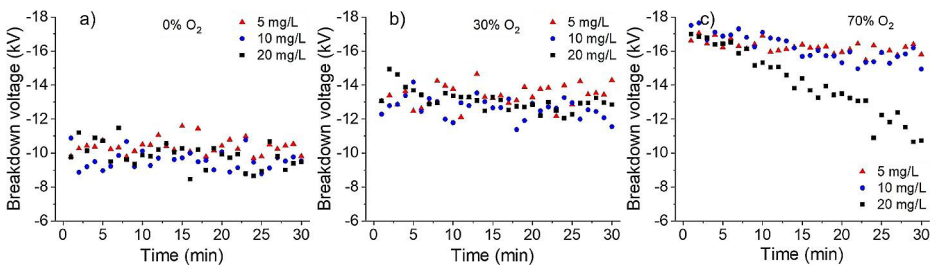


Fig. 5 Evolution of breakdown voltage as a function of plasma processing time of deionized water with MB at different initial concentration (5, 10, and 20 mg/L) under different conditions of O₂ percentage in Ar: (a) 0%, (b) 30%, and (c) 70%

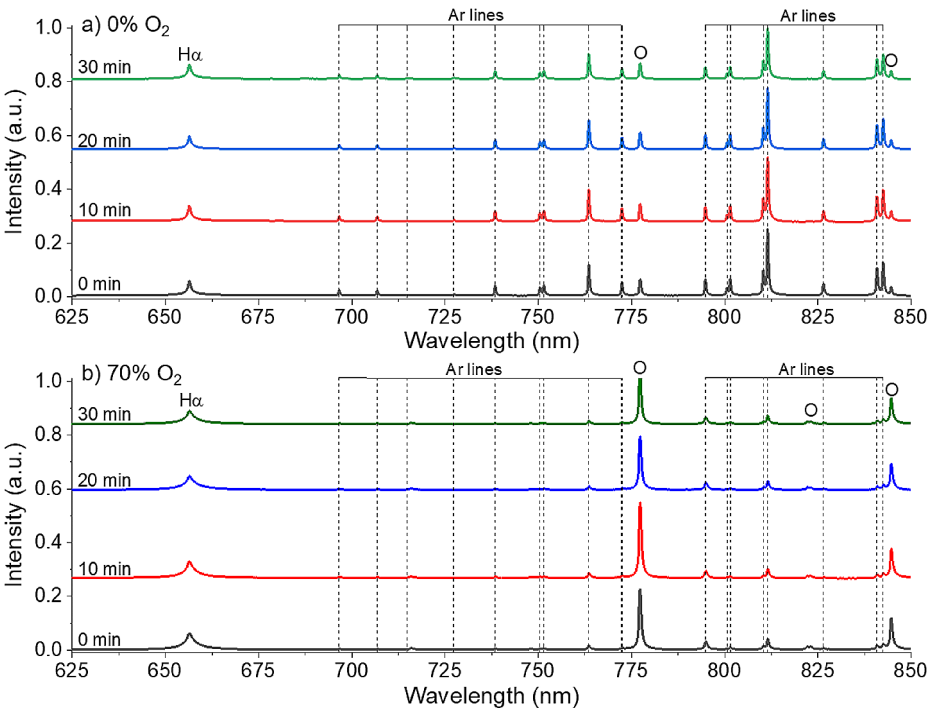


Fig. 6 Evolution of optical emission spectra as a function of plasma processing time of deionized water with MB at 10 mg/L under different conditions of O₂ percentage in Ar: (a) 0% and (b) 70%

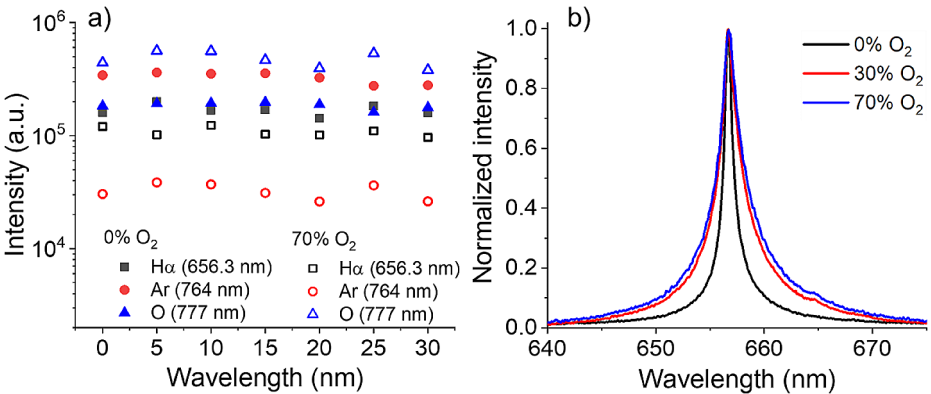


Fig. 7 a) Evolution of emission intensity of H α , Ar, and O as a function of plasma processing time of deionized water with MB at 10 mg/L under different conditions of O₂ percentage in Ar (0% and 70%). b) Normalized H α line acquired with different percentage of O₂

The evolution of the intensity of H α (at 656.3 nm), Ar (at 764 nm), and O (at 777 nm) lines as a function of plasma processing time is shown in Fig. 7a for 0% and 70% O₂. The results show that there is no significant evolution of the emission lines. This finding is of interest as it means that the plasma properties did not change with the processing time,

despite the fact the MB is completely degraded after 30 min of processing. In fact, the utilization of Ar and Ar-O₂ mixture as bubble composition did not generously produce ionic species with long lifetimes, as the highest solution electrical conductivity ($\sim 40\text{--}50\ \mu\text{S}/\text{cm}$) was measured with 70% O₂ (in N₂ gas the conductivity increases to few hundreds of $\mu\text{S}/\text{cm}$ [24] due to the production of nitrate and nitrite species in solution which modifies the discharge properties). On the other hand, the profile of H α line did not change with the processing time, but it depends on the O₂ content. For instance, the broader H α line is obtained with 70 and 30% of O₂, which indicates higher electron density when O₂ is added. This finding further agrees with the higher breakdown voltage and higher discharge current measured under these conditions.

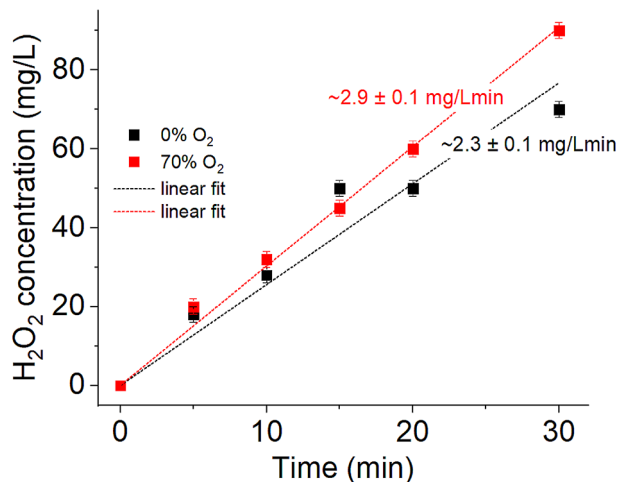
Figure 8 shows the H₂O₂ concentration produced in 0% O₂ and 70% O₂ plasmas as a function of time. In the 0% O₂ plasma, H₂O₂ concentration reaches $\sim 70\ \text{mg}/\text{L}$ after 30 min of processing, while in the 70% O₂ plasma, H₂O₂ concentration reaches $\sim 90\ \text{mg}/\text{L}$ after the same time of processing. In both conditions, the concentration increases linearly with processing time with a rate of $\sim 2.3 \pm 0.1\ \text{mg}/\text{Lmin}$ in the 0% O₂ plasma and $\sim 2.9 \pm 0.1\ \text{mg}/\text{Lmin}$ in the 70% O₂ plasma.

Production of H₂O₂ in discharges in contact with liquids is generally attributed to the recombination of two OH radicals, i.e. $\text{OH} + \text{OH} \rightarrow \text{H}_2\text{O}_2$ [29]. Thus, the higher H₂O₂ concentrations and reaction rate in an O₂-containing discharge also indicates a higher production of OH radicals in Ar-O₂ plasma. Since electron dissociation of the water molecule is known as a major reaction for OH radical production [30], this is coherent with the higher breakdown voltage and electron densities in those conditions, as reported earlier by the electrical and optical characterization.

Plasma Induced Degradation of Methylene Blue (MB)

MB is used as a representative organic contaminant of water, and its degradation rate was determined under different conditions of gas composition, namely at different O₂ content in Ar, MB concentration, and water electrical conductivity. The MB degradation rate was monitored using UV-visible absorption spectroscopy. Figure 9 shows the evolution of the absorption spectra for different plasma processing times. Representative MB absorption

Fig. 8 H₂O₂ concentration as a function of plasma processing time in deionized water under different conditions of O₂ percentage in Ar (0% and 70%)



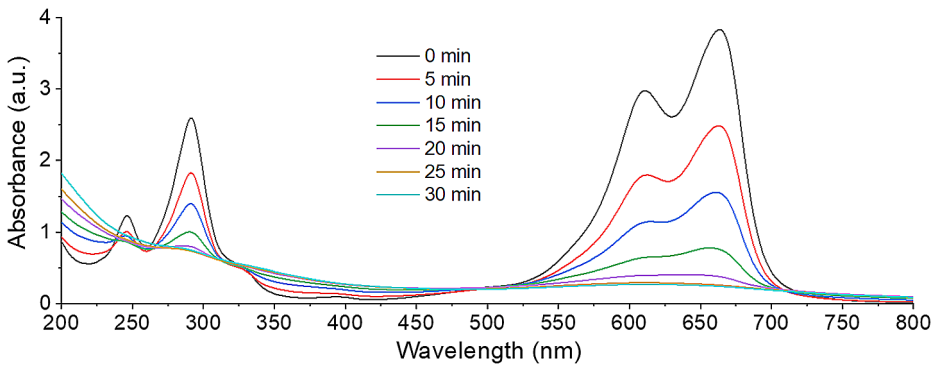


Fig. 9 Evolution of the absorbance spectrum of MB deionized water with MB (at 10 mg/L) as a function of plasma processing with 30% O₂ of gas composition

peaks are observed at 664, 292, and 246 nm and are respectively associated with the auxochrome group, the conjugated system of phenothiazine, and the benzene ring [24]. The decrease of these peaks with treatment time (Fig. 9) indicates the successful degradation of MB induced by plasma. In addition, at 400 nm, we see a continuum of absorbance that its value increases for shorter wavelengths and for longer treatment time. In general, absorbance in the visible range is associated with conjugated (i.e. consecutive) pi bonds for which the orbitals have a lower energy gap. Therefore, a shift in absorbance from visible to UV wavelengths can be attributed to the presence of molecules with fewer conjugated pi bonds and more unconjugated pi bonds [31]. This indicates that the plasma species successfully decomposed MB molecules in shorter products. In the following Sections, the effects of different discharge conditions on the degradation rate of MB are discussed based on the intensity of the peak at 664 nm.

Figure 10a shows the evolution of the normalized absorbance (at 664 nm) as a function of plasma processing time with different percentage of O₂. The results show that the efficiency of MB degradation increases with O₂ content. Figure 10b shows the variation of plasma processing time needed to degrade 50% ($t_{50\%}$) of MB in solution as a function of O₂ content. $t_{50\%}$ decreases linearly from ~12.5 to 4.5 min as O₂ content increases from 0 to 50%. Further increase of O₂ content did not significantly influences $t_{50\%}$. These results are consequent with previous experiments in Ar and O₂ discharges [24, 25], where the higher degradation in O₂ was attributed to a higher fluence of reactive oxygen species.

Figure 11 shows the evolution of the normalized absorbance (at 664 nm) as a function of plasma processing time of deionized water with MB at different initial concentration, namely 5, 10, and 20 mg/L, and under different percentage of O₂ content in Ar (0%, 30%, and 70%). At 0% O₂, the degradation of 5-mg/L-concentrated solution is faster than the other solutions (at 10 and 20 mg/L). For instance, $t_{50\%}$ is ~7 min at 5-mg/L-solution and ~12.5 min for the other solutions. Also, one remarks that the absorbance decrease of the less concentrated solution is faster during the first 15 min of processing, but the absorbance measured during the first 5 min for the other solutions is slower and becomes comparable after this period. At 30% O₂, the data behavior is similar to the 0% O₂ case, but the degradation is faster ($t_{50\%}$ = 4 min for 5 mg/L and 8 min for 10 and 20 mg/L solutions). At 70% O₂, the degradation is even faster ($t_{50\%}$ = 3, 4, and 5 min for 5, 10, and 20 mg/L solutions,

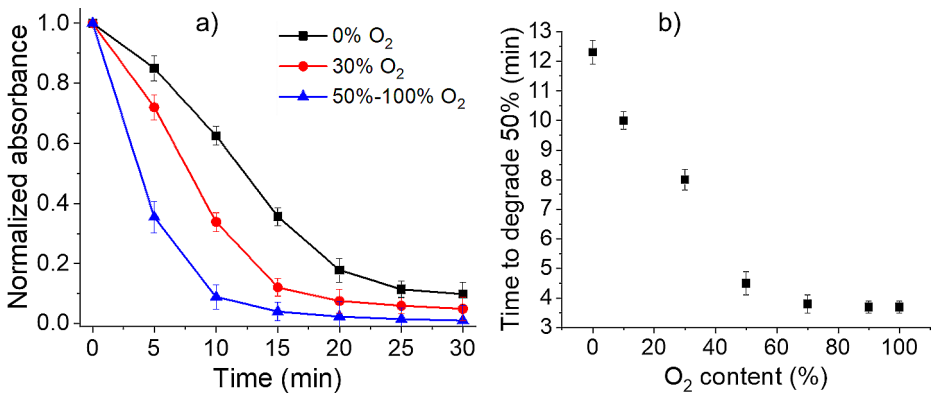


Fig. 10 a) Evolution of the normalized absorbance (at 664 nm) of MB solution (10 mg/L) as a function of plasma processing under different conditions of O₂ content in Ar. b) Variation of processing time needed to degrade 50% of MB as a function of O₂ content

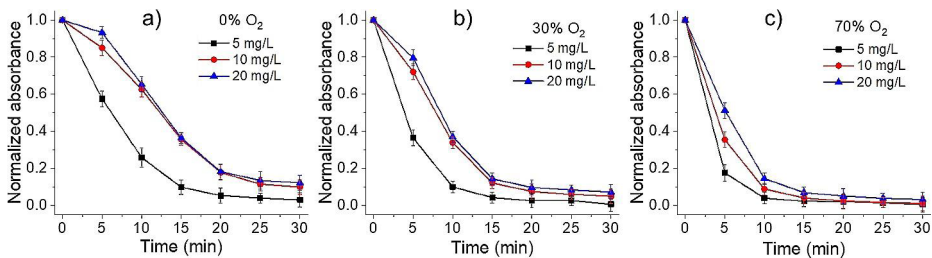


Fig. 11 Evolution of the normalized absorbance (at 664 nm) as a function of plasma processing time of deionized water with MB at different initial concentration (5, 10, and 20 mg/L) under different conditions of O₂ percentage in Ar: (a) 0%, (b) 30%, and (c) 70%

respectively), and the degradation starts with the faster rate from the very beginning for the three solutions. Finally, we note that a complete degradation (absorbance ~ 0) is obtained for the 5 mg/L solution in the three O₂ conditions, but for the other concentrations (10 and 20 mg/L), a complete degradation is obtained only at high O₂ content. Since the pictured absorbance is normalized to the initial MB concentration, a change in the MB degradation rate indicates a change in the implicated chemical kinetics. Such a change could be explained by a saturation of the treatment where not enough ROS are generated, which limits the number of MB molecules that can be simultaneously treated at 10 and 20 mg/L. However, at low MB concentration of 5 mg/L, the higher absorbance rate indicates a transition to a higher order of chemical kinetics, where the MB concentration influences the reaction rate. When O₂ is added to the gas mixture, a higher number of ROS is expected. Consequently, the MB degradation is not saturated by a limited number of ROS, which can explain why the curves on Fig. 11 are less affected when the initial MB concentration varies from 5 to 20 mg/L.

Figure 12 shows the evolution of the normalized absorbance (at 664 nm) as a function of plasma processing time of water with MB (5 mg/L) and at different electrical conductivities, namely 5, 50, 100, and 200 $\mu\text{S}/\text{cm}$. The processing is conducted at different conditions of O₂

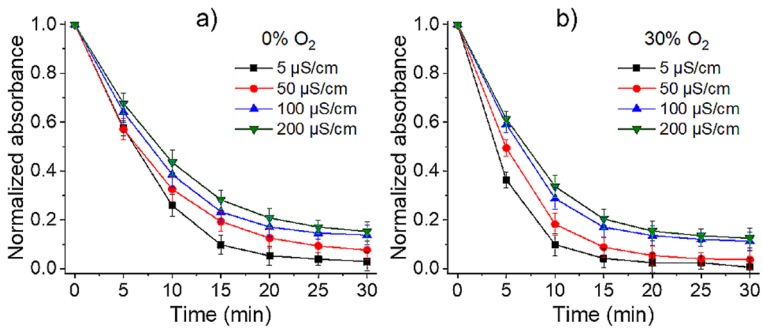


Fig. 12 Evolution of the normalized absorbance (at 664 nm) as a function of plasma processing time of water with MB (5 mg/L) and at different electrical conductivities. The processing is conducted at different conditions of O₂ percentage in Ar: (a) 0% and (b) 30%

percentage in Ar, namely 0% (Fig. 12a) and 30% (Fig. 12b). In both cases, we observe that the increase of water electrical conductivity reduces the efficiency of the plasma to induce MB degradation. For instance, at 0% O₂, $t_{50\%}$ is ~6 and 9 min at 5 and 200 $\mu\text{S}/\text{cm}$, respectively, whereas at 30% O₂, $t_{50\%}$ is ~4 and 7.5 min at 5 and 200 $\mu\text{S}/\text{cm}$, respectively. The reduction in efficiency is related to the modifications of the discharge electrical characteristics (i.e. discharge properties), namely a decrease in the discharge current by few amperes, a decrease of the probability of discharge occurrence (by 10–20%), and an increase of the discharge delay (by ~100 ns), which indicates the occurrence of the discharges later in the pulse, i.e. a plasma with shorter lifetime and lower energy (Figure S2 in Supplementary Material).

The above-mentioned findings clearly highlight that Ar-O₂ gas mixture significantly influences the discharge characteristics as well as the MB degradation rate. The electrical characteristics showed that the addition of Ar to O₂ reduces the breakdown voltage by several kilovolts. This phenomenon is attributed to the decrease of the reduced critical E-field strength [28]; this latter is due to the decrease of the concentration of O-species, i.e. lower rate of electron loss by attachment to form O⁻ and O₂⁻. We also find that MB degradation is significantly enhanced by adding O₂ to Ar up to 50%. Higher O₂ content did not enhance the degradation further. This can be explained by a competition between the increase of ROS production and the decrease of the discharge efficiency (i.e. lower injected energy as the discharges ignite later in the pulse, Fig. 4c). These results show that the control of Ar-O₂ gas mixture can be utilized to optimize the reactor performance, i.e. maximize the MB degradation and minimize the energy consumption.

Scale up: A Setup with Four Electrodes

In this section, we aim to have a step towards scaling up the setup. For this purpose, the number of electrodes is increased to four, i.e. four plasma zones are obtained. The four needles were all connected to the high voltage, whereas the grounded electrode was a stainless-steel wire (1 mm diameter) placed at 8 mm above the needles (Fig. 13). The volume of the MB solution was 300 mL. The cylindrical cell was filled with 200 mL, meanwhile the remaining 100 mL is filled in a cell where the measurements of liquid properties (acidity, conductivity, and MB absorbance) are performed. Two pumps (Ismatec™ MS-2/6 Reglo Analog Pump)

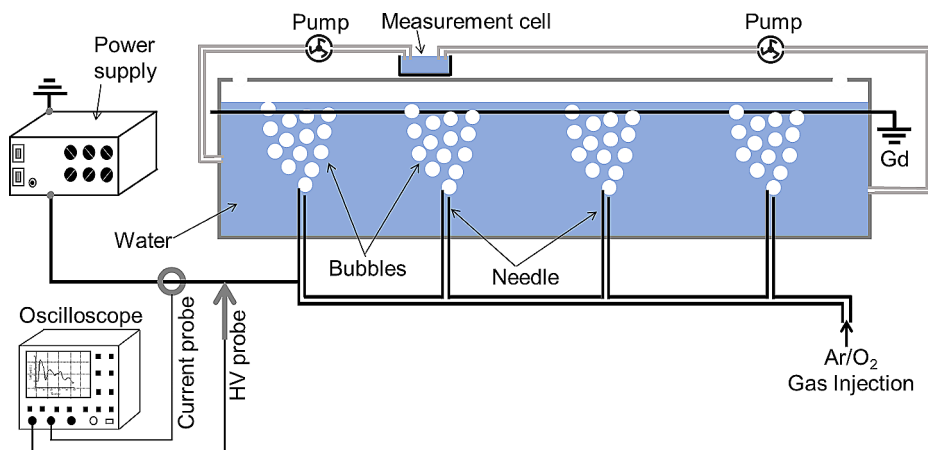


Fig. 13 Scheme of the experimental setup composed of four electrodes

were utilized at a flow rate of 50 mL/min to ensure circulation of the solution. The discharge parameters were the same of the one electrode setup (frequency = 1 kHz, voltage = -20 kV, pulse width = 500 ns, and gas flow rate = 4 L/min).

Initially, we run the discharges with 100% Ar or 100% O₂ at a flow rate of 4 L/min, so a flow of 1 L/min (same as in the one electrode setup) per needle is expected. The electrical characteristics, voltage and current, were very similar to the case of one electrode setup (the data are not shown). This is expected as they were measured across the four electrodes. In the case of Ar, the temporal evolution of breakdown voltage and discharge current were not significant. However, we noticed that the probability of discharge occurrence diminishes especially after 25 min of processing. In the case of O₂ gas, we also observed a decrease in the probability of discharge occurrence as a function of processing time, as well as a decrease of the breakdown voltage (from ~-17 to -14 kV) and a decrease of the discharge current peak (from ~-41 to -39 A) after 30 min of processing. This decrease was observed in the one electrode setup, and it was attributed to the increase of the electrical conductivity of the solution. Interestingly, we observed that the breakdown voltage decreases by the same value ($\Delta V = 3$ kV) in both configurations (one and four electrodes setups) despite the fact that the increase of the solution conductivity is much higher in the one electrode setup. For instance, after 30 min of processing, it increases from ~5 to 50 $\mu\text{S/cm}$ in the one setup and from ~5 to 27 $\mu\text{S/cm}$ in the four electrodes setup. At this stage, we believe that this behaviour could be an indicator that the configuration with multiple electrodes is more sensitive to solution conductivity.

We also monitored the plasma emission in the four electrodes setup (at one electrode), and the acquired spectra showed emission lines similar to those acquired in the one electrode setup, but the intensity was lower.

The concentration of H₂O₂ was also measured in the four electrodes setup with 0% and 100% O₂ gas, and the results are shown in Fig. 14. In both gases, H₂O₂ concentration increases linearly with the processing time to reach ~54 and ~36 mg/L after 30 min of processing in the case of 100% O₂ and 0% O₂, respectively. H₂O₂ production rate in the four electrodes setup is thus estimated by $\sim 1.2 \pm 0.1$ mg/Lmin in 0% O₂ and $\sim 1.9 \pm 1$ mg/Lmin in 100% O₂; compared to the one electrode setup, H₂O₂ production rate is reduced by fac-

Fig. 14 H₂O₂ concentration in multi needles configuration as a function of plasma processing time in deionized for with 100% Ar and 100% O₂

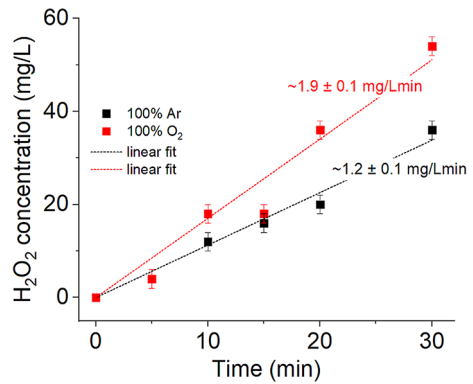
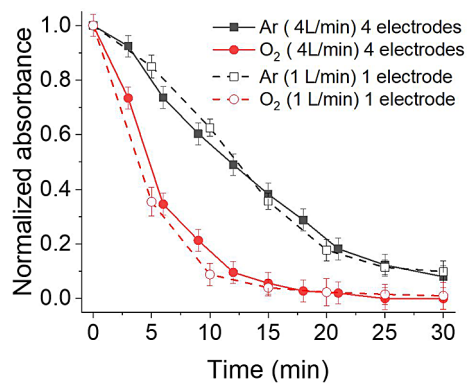


Fig. 15 MB degradation rate under different conditions using 0% and 100% O₂ at a gas flow rate of 4 L/min; the data obtained in one electrode setup (1 L/min) are added to the figure



tors of ~2 and 1.6 in 0% and 100% O₂, respectively. The reduction of efficiency in H₂O₂ production in the four electrodes setup can be explained by the fact that when increasing the number of electrodes, the current and power density across one electrode decrease, which reduces the amount of produced OH in solution. Therefore, the quantity of H₂O₂ formed by OH recombination is also reduced [32, 33].

The four electrodes setup was tested to degrade MB at initial concentration of 10 mg/L with 0% and 100% O₂ at a gas flow rate of 4 L/min (Fig. 15). The data were superimposed to those obtained in the one electrode setup and, interestingly, there is a great accordance. This finding is of interest as it may suggest the feasibility of scaling up of the setup.

Figure 16 shows the performance of the four electrodes setup in the degradation of MB at various initial concentrations (5, 10, and 20 mg/L). The experiments were conducted in 100% O₂ conditions at a flow rate of 4 L/min. The data are superimposed to those obtained in the one electrode setup. As it can be seen in the figure, the MB degradation rates obtained in both setups are comparable in the case of 5 and 10 mg/L, but the setup with four electrodes is less efficient in the case of 20 mg/L. This difference can be linked to the low production rate of OH in the four electrodes setup, as evidenced by the lower concentration of H₂O₂ (Figs. 8 and 14).

Figure 17 represents the evolution of the normalized absorbance at 664 nm of MB (initial concentration of 10 mg/L) solution at different electrical conductivities (5, 50, 100, and 200 μS/cm). Here also, a 100% O₂ was used at a flow rate of 4 L/min. The results clearly

Fig. 16 Evolution of the normalized absorbance (at 664 nm) as a function of plasma processing time of deionized water with MB at different initial concentration (5, 10, and 20 mg/L) using O₂ at gas flow rate of 4 L/min; the data obtained in one electrode setup (1 L/min) are added to the figure

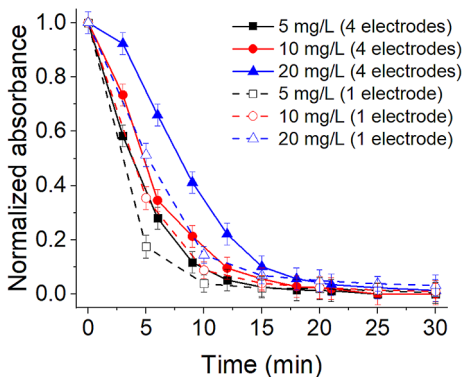
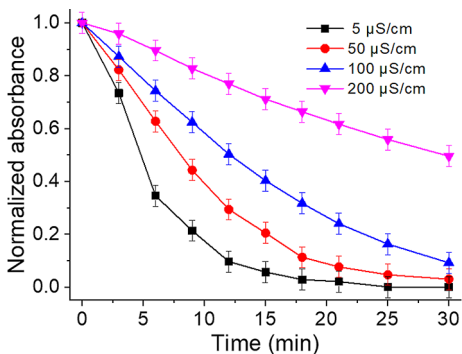


Fig. 17 Evolution of the normalized absorbance (at 664 nm) as a function of plasma processing time of water with MB (10 mg/L) and at different electrical conductivities. The processing is conducted with O₂ at 4 L/min



show that increasing the electrical conductivity of the solution significantly decreases the degradation rate of MB. As compared to the one electrode setup, the reduction in efficiency in the four electrodes setup is more significant. We believe that this decrease in degradation efficiency is related to the fact that discharge current (or the power) is distributed to four electrodes instead of one. This makes the discharge occurrence highly sensitive to the electrical conductivity of the solution, and the probability of discharge occurrence is significantly reduced at higher conductivity and longer processing time.

The results obtained in the four electrodes setup were unexpected. In terms of H₂O₂ production rate, a reduction by a factor of ~1.6–2.0, depending on the gas composition, is obtained. Such a reduction can be explained by a lower current and power density due to the increased number of electrodes. At low initial MB concentration and low electrical conductivity, the efficiency of both setups to degrade MB was comparable, which indicates the feasibility of the scale up. However, at high electrical conductivity and high initial MB concentration, the reactor with four electrodes becomes less efficient than that of one electrode. These findings are of interest, as they highlight a challenging issue facing the scaling up. Indeed, the sensitivity of the reactor to certain parameters (e.g. initial pollutant concentration, solution properties, input power, etc.) requires a special attention when large scale reactors are designed.

Energy Efficiency

The energy yield $Y_{50\%}$ represents the amount of the eliminated contaminant per unit of delivered energy at 50% degradation of the pollutant, and it is expressed by the following equation [34]:

$$Y_{50\%}(g/kWh) = \frac{V \times C_0 \times \frac{C_0 - C}{C_0}}{P \times t} \tag{1}$$

where $V(L)$ is the volume of treated solution, $C_0(g/L)$ is the initial concentration of MB solution, $C(g/L)$ is the concentration of MB solution after 50% degradation, $P(kW)$ is the input power, $t(h)$ is the treatment time to reach 50% of MB conversion.

As it considers several parameters, $Y_{50\%}$ is suitable to assess and compare the reactors performance working under different operating conditions. Table 1 provides the values of $Y_{50\%}$ under different operating conditions for the one and the four electrodes setups. To properly estimate the power, two methods are considered. The first method consists of calculating the power from the electrical, voltage and current, waveforms. Despite the dependence of the waveforms on the experimental conditions, a value of ~20 W is estimated. On the other hand, we measured the power dissipated by the whole experiment; this was determined by adding a monitor at the wall plug where the equipment was connected. The total consumed power was 181 W. The obtained $Y_{50\%}$ for the two power values are added to the table. Interestingly, if we consider only the power dissipated by the discharge a yield that is ~10 time higher than the case when the total power consumption is considered. For instance, the highest $Y_{50\%}$ is obtained in the case of 20 mg/L of MB concentration at low electrical conductivity with 70% O₂. When considering the total power, we determine $Y_{50\%}$ of ~133 mg/kWh, while when the discharge power is considered, we obtain $Y_{50\%}$ of 1263 mg/kWh.

Table 1 Summary of the $Y_{50\%}$ determined in the one and the four electrodes setups under the various experimental conditions

Configuration	Gas composition	C_0 (mg/L)	σ ($\mu S/cm$)	$t_{50\%}$ (min)	$Y_{50\%}$ (mg/kWh) \pm $\Delta Y_{50\%}$	
					$P=181$ W	$P=20$ W
One electrode setup Flow rate= 1 L/min	100% Ar+0% O ₂	10	5	12.5	27 \pm 1	252 \pm 1
	30% Ar+70% O ₂	10	5	4.5	74 \pm 3	701 \pm 3
		5	5	3	55 \pm 3	526 \pm 3
		20	5	5	133\pm4	1263\pm4
	100% Ar+0% O ₂	5	5	6	28 \pm 2	263 \pm 2
		5	200	9	18 \pm 1	175 \pm 1
70% Ar+30% O ₂	5	5	4	41 \pm 3	394 \pm 3	
	5	200	7.5	22 \pm 1	210 \pm 1	
Four electrodes setup Flow rate= 4 L/min	100% Ar+0% O ₂	10	5	12	41 \pm 2	394 \pm 2
	0% Ar+100% O ₂	10	5	5	99 \pm 4	947 \pm 4
		5	5	4	62 \pm 4	592 \pm 4
		20	5	8	124\pm4	1184\pm4
		10	200	30	17 \pm 1	157 \pm 1

From the table above and when the total power is considered, $Y_{50\%}$ in the one electrode setup varies from 18 to 133 mg/kWh; the highest yield is obtained at 70% O_2 for 20 mg/L initial concentration solution in deionized water. In the four electrodes setup, $Y_{50\%}$ ranges between 17 and 124 mg/kWh; the highest yield is obtained when O_2 is used for 20 mg/L initial MB concentration in deionized water. In the four electrodes setup, we found that $Y_{50\%}$ (41 and 99 mg/kWh in Ar and O_2 , respectively) is relatively higher than in the one electrode setup (27 and 74 mg/kWh in Ar and O_2 , respectively). This result can be explained as follows: since the four electrodes setup contains more discharge zones, the plasma-liquid interface is therefore enhanced leading to efficient transfer of reactive species from the discharge zone to the solution.

In the cases of various MB concentrations, namely 5, 10, and 20 mg/L, when O_2 gas is used, we observed that $Y_{50\%}$ in the four electrodes setup is relatively higher (62 and 99 mg/kWh at 5 and 10 mg/L, respectively) than that in the one electrode setup (55 and 74 mg/kWh at 5 and 10 mg/L, respectively). However, at 20 mg/L, $Y_{50\%}$ in the one electrode setup is slightly higher than that in the four electrodes setup (133 vs. 124 mg/kWh). These results indicate that for low MB concentration (<10 mg/L), the scale up is effective as the four electrodes setup showed better performance. However, for high MB concentration, the one electrode setup is more efficient.

Concerning the electrical conductivity of the solution, we found that increasing it reduces the energy efficiency in both setups. In the case of deionized water (5 $\mu\text{S}/\text{cm}$), $Y_{50\%}$ in the four electrodes setup (99 mg/kWh) is significantly higher than that in the one electrode setup (28 and 41 mg/kWh at 0% and 30% O_2 , respectively). However, at 200 $\mu\text{S}/\text{cm}$, $Y_{50\%}$ in the four electrodes setup drops dramatically to reach 17 mg/kWh, and it is comparable to that found in the one electrode configuration (18 and 22 mg/kWh at 0% and 30% O_2 , respectively).

At this stage, it is possible to compare the results found herein with those reported in literature (Table S1 in Supplementary Material). In general, most of the reactors utilized to degrade MB reported $Y_{50\%}$ between ~ 37 and 1500 mg/kWh [4–6, 8, 34–38]. We believe that these values are determined using the power dissipated in the discharge and not the total power consumed by the equipment. Therefore, to compare the $Y_{50\%}$ determined herein, we must use the values deduced from the power dissipated by the discharge. In this case, $Y_{50\%}$ varies between 157 and 1263 mg/kWh. These values are comparable with those reported in the literature.

Finally, we would like to end this study with the statement that it is unlikely to design a single reactor capable of removing different kinds of pollutants present in different kinds of waters. We believe that the future of plasma technology in water depollution will be based on the optimization of a given reactor for a given pollutant present in water.

Conclusion

This study analyzes the degradation of methylene blue (MB) using pulsed discharges in gas bubbles in water. The electrical and optical characteristics of the discharge in Ar plasma stay stable with time, even when MB is added to the water. When high O_2 content (70%) is present in the Ar- O_2 gas mixture, the electrical characteristics vary slightly with time, which is due to the gradual incorporation of ionic species in solution. The efficacy of the discharge

to produce H_2O_2 is evaluated, and its production rate was evaluated to ~ 2.3 and 2.9 mg/Lmin in 0% and 70% O_2 gas, respectively.

The degradation of MB was evaluated using one and four electrodes' setups. In the one electrode setup, the degradation efficiency increased when adding O_2 to Ar gas, and a plateau is reached if % $O_2 > 70\%$. The effect of water electrical conductivity (up to $200 \mu S/cm$) is assessed, and we found a decrease in degradation efficiency at higher conductivity.

In the four electrodes setup, the results showed that the electrical and the optical characteristics had similar behaviour as the single needle configuration, but the production rate of H_2O_2 is reduced by a factor of ~ 2 and 1.6 in 0% and 100% O_2 , respectively. On the other hand, we observed that at low MB concentration and electrical conductivity, the performance of the four electrodes setup is higher, whereas, at high MB concentration, the one electrode setup seems to have better performance. We also found that the performance of the four electrodes setup is dramatically degraded as the conductivity of the solution is increased, indicating thus a great sensitivity of the discharge on conductivity in the four electrodes setup.

Supplementary Information The online version contains supplementary material available at <https://doi.org/10.1007/s11090-024-10468-6>.

Acknowledgements The research reported in this publication was financially supported by the Natural Sciences and Engineering Research Council of Canada (NSERC), under award number RGPIN-2023-03951. The authors thank the Fonds de Recherche du Québec – Nature et Technologie (FRQ-NT) and the Canada Foundation for Innovation (CFI) for funding the research infrastructure.

Author Contributions N A, J P, and A H wrote the main manuscript text and prepared the Figures. C G, N A, and J P did the experiments under the supervision of A H. N A, J P, A H, and I B contributed to the writing and revision of the manuscript. All authors reviewed the manuscript.

Funding This work was financially supported by the National Science and Engineering Research Council (NSERC), under award numbers RGPIN-2023-03951.

Data Availability No datasets were generated or analysed during the current study.

Declarations

Ethical Approval Not applicable.

Competing Interests The authors declare no competing interests.

References

1. Hassaan MA, Nemr E, A., Hassaan A (2017) Health and environmental impacts of dyes: mini review. *Am J Environ Sci Eng* 1(3):64–67
2. Manzoor J, Sharma M (2020) Impact of textile dyes on human health and environment. *Impact of textile dyes on public health and the environment*. IGI Global, pp 162–169
3. Magureanu M, Mandache NB, Parvulescu VI (2007) Degradation of organic dyes in water by electrical discharges. *Plasma Chem Plasma Process* 27:589–598
4. Hamdan A, Liu JL, Cha MS (2018) Microwave plasma jet in water: characterization and feasibility to wastewater treatment. *Plasma Chem Plasma Process* 38:1003–1020

5. Diamond J, Profili J, Hamdan A (2019) Characterization of various air plasma discharge modes in contact with water and their effect on the degradation of reactive dyes. *Plasma Chem Plasma Process* 39:1483–1498
6. Krosuri A, Wu S, Bashir MA, Walquist M (2021) Efficient degradation and mineralization of methylene blue via continuous-flow electrohydraulic plasma discharge. *J Water Process Eng* 40:101926
7. Magureanu M, Piroi D, Mandache NB, David V, Medvedovici A, Parvulescu VI (2010) Degradation of pharmaceutical compound pentoxifylline in water by non-thermal plasma treatment. *Water Res* 44(11):3445–3453
8. Malik MA, Ghaffar A, Ahmed K (2002) Synergistic effect of pulsed corona discharges and ozonation on decolourization of methylene blue in water. *Plasma Sources Sci Technol* 11(3):236
9. Magureanu M, Bradu C, Piroi D, Mandache NB, Parvulescu V (2013) Pulsed corona discharge for degradation of methylene blue in water. *Plasma Chem Plasma Process* 33:51–64
10. Lukes P, Appleton AT, Locke BR (2004) Hydrogen peroxide and ozone formation in hybrid gas-liquid electrical discharge reactors. *IEEE Trans Ind Appl* 40(1):60–67
11. Hsieh KC, Wang H, Locke BR (2016) Analysis of Electrical Discharge plasma in a gas-liquid Flow Reactor using Optical Emission Spectroscopy and the formation of Hydrogen Peroxide. *Plasma Processes Polym* 13(9):908–917
12. Sahni M, Locke BR (2006) Quantification of hydroxyl radicals produced in aqueous phase pulsed electrical discharge reactors. *Industrial& Eng Chemistryresearch* 45(17):5819–5825
13. Lukes P, Clupek M, Babicky V, Janda V, Sunka P (2005) Generation of ozone by pulsed corona discharge over water surface in hybrid gas–liquid electrical discharge reactor. *J Phys D* 38(3):409
14. Baroch P, Anita V, Saito N, Takai O (2008) Bipolar pulsed electrical discharge for decomposition of organic compounds in water. *J Electrostat* 66(5–6):294–299
15. Sugiarto AT, Ito S, Ohshima T, Sato M, Skalny JD (2003) Oxidative decoloration of dyes by pulsed discharge plasma in water. *J Electrostat* 58(1–2):135–145
16. Dang TH, Denat A, Lesaint N, Teissedre G (2009) Pulsed electrical discharges in water for removal of organic pollutants: a comparative study. *Eur Phys Journal-Applied Phys* 47(2):22818
17. El Shaer M, Eldaly M, Heikal G, Sharaf Y, Diab H, Mobasher M, Rousseau A (2020) Antibiotics degradation and bacteria inactivation in water by cold atmospheric plasma discharges above and below water surface. *Plasma Chem Plasma Process* 40:971–983
18. Matsui Y, Takeuchi N, Sasaki K, Hayashi R, Yasuoka K (2011) Experimental and theoretical study of acetic-acid decomposition by a pulsed dielectric-barrier plasma in a gas–liquid two-phase flow. *Plasma Sources Sci Technol* 20(3):034015
19. Magureanu M, Piroi D, Gherendi F, Mandache NB, Parvulescu V (2008) Decomposition of methylene blue in water by corona discharges. *Plasma Chem Plasma Process* 28:677–688
20. Nishiyama H, Niinuma K, Shinoki S, Takana H (2015) Decomposition of acetic acid using multiple bubble jets with pulsed electrical discharge. *Plasma Chem Plasma Process* 35:339–354
21. Chen YS, Zhang XS, Dai YC, Yuan WK (2004) Pulsed high-voltage discharge plasma for degradation of phenol in aqueous solution. *Sep Purif Technol* 34(1–3):5–12
22. Shih KY, Locke BR (2010) Chemical and physical characteristics of pulsed electrical discharge within gas bubbles in aqueous solutions. *Plasma Chem Plasma Process* 30:1–20
23. Wright A, Taglioli M, Montazersadgh F, Shaw A, Iza F, Bandulasena HH (2019) Microbubble-enhanced DBD plasma reactor: design, characterisation and modelling. *Chem Eng Res Des* 144:159–173
24. Bourbeau N, Soussan L, Hamdan A (2022) Degradation of methylene blue by pulsed nanosecond discharge in Ar, O₂, and N₂ gaseous bubbles in water: evaluation of direct and postprocessing modes. *J Vacuum Sci & Technology A*, 40(5)
25. Sun B, Sato M, Clements JS (1999) Use of a pulsed high-voltage discharge for removal of organic compounds in aqueous solution. *Journal of Physics D: Applied Physics*, 32(15), 1908
26. Zhang Y, Zhou M, Hao X, Lei L (2007) Degradation mechanisms of 4-chlorophenol in a novel gas–liquid hybrid discharge reactor by pulsed high voltage system with oxygen or nitrogen bubbling. *Chemosphere* 67(4):702–711
27. Grabowski LR, Van Veldhuizen EM, Pemen AJM, Rutgers WR (2007) Breakdown of methylene blue and methyl orange by pulsed corona discharge. *Plasma Sources Sci Technol* 16(2):226
28. Talviste R, Erme K, Paris P, Raud J, Plank T, Jõgi I (2022) Effective ionization coefficient in mixtures of ar and O₂ determined using the Townsend discharge. *AIP Adv*, 12(10)
29. Locke BR, Shih KY (2011) Review of the methods to form hydrogen peroxide in electrical discharge plasma with liquid water. *Plasma Sources Sci Technol* 20(3):034006
30. Magureanu M, Bradu C, Parvulescu VI (2018) Plasma processes for the treatment of water contaminated with harmful organic compounds. *J Phys D* 51(31):313002
31. <https://www.masterorganicchemistry.com/2016/09/16/introduction-to-uv-vis-spectroscopy/>

32. Sugai T, Nguyen PT, Maruyama T, Tokuchi A, Jiang W (2016) The effect of scale-up of pulsed corona discharge for treatment of pollution water sprayed in discharge gap. *IEEE Trans Plasma Sci* 44(10):2204–2210
33. Liu ZJ, Wang WC, Zhang L, Wang S, Yang DZ, Zhang S, Tang K (2014) Electrical and optical characteristics of diffuse nanosecond pulsed discharge plasma using a needle-array electrode in atmospheric air. *J Appl Phys*, 115(20)
34. García MC, Mora M, Esquivel D, Foster JE, Rodero A, Jiménez-Sanchidrián C, Romero-Salguero FJ (2017) Microwave atmospheric pressure plasma jets for wastewater treatment: degradation of methylene blue as a model dye. *Chemosphere* 180:239–246
35. Stará Z, Krěma F, Nejezchleb M, Skalný JD (2009) Organic dye decomposition by DC diaphragm discharge in water: Effect of solution properties on dye removal. *Desalination* 239(1–3):283–294
36. Ikoma S, Satoh K, Itoh H (2009) Decomposition of methylene blue in an aqueous solution using a pulsed-discharge plasma at atmospheric pressure. *IEEJ Trans Fundamentals Mater* 129(4):237–244
37. Ishijima T, Hotta H, Sugai H, Sato M (2007) Multibubble plasma production and solvent decomposition in water by slot-excited microwave discharge. *Appl Phys Lett*, 91(12)
38. Maehara, T., Miyamoto, I., Kurokawa, K., Hashimoto, Y., Iwamae, A., Kuramoto, M.,... Kawashima, A. (2008). Degradation of methylene blue by RF plasma in water. *Plasma Chemistry and Plasma Processing*, 28, 467–482

Publisher's Note Springer Nature remains neutral with regard to jurisdictional claims in published maps and institutional affiliations.

Springer Nature or its licensor (e.g. a society or other partner) holds exclusive rights to this article under a publishing agreement with the author(s) or other rightsholder(s); author self-archiving of the accepted manuscript version of this article is solely governed by the terms of such publishing agreement and applicable law.

Authors and Affiliations

Nadir Aloui^{1,2} · Julien Pregent^{3,4} · Camille Gouze¹ · Ibtissem Belgacem² · Ahmad Hamdan¹

✉ Ahmad Hamdan
ahmad.hamdan@umontreal.ca

- ¹ Groupe de physique des plasmas, Département de Physique, Université de Montréal, 1375 Avenue Thérèse-Lavoie-Roux, Montréal, Québec H2V 0B3, Canada
- ² Laboratoire de Recherche des sciences de l'eau, Département Hydraulique, École Nationale Polytechnique. 10, Rue des frères OUDEK, El Harrach 16200, Alger, Algérie
- ³ Département de physique, Cégep de Saint-Laurent, 625 Avenue Sainte-Croix, Saint-Laurent, Québec H4L 3X7, Canada
- ⁴ Centre des technologies de l'eau, 696 Avenue Sainte-Croix, Saint-Laurent, Québec H4L 3Y2, Canada